

**The Oxford Classic links epithelial-mesenchymal transition to immunosuppression in poor prognosis ovarian cancers**

Zhiyuan Hu <sup>1,2,#</sup>, Paula Cunnea <sup>3,#</sup>, Zhe Zhong <sup>1,2,4</sup>, Haonan Lu <sup>3,12</sup>, Oloruntoba I. Osagie <sup>1,2</sup>, Leticia Campo <sup>5</sup>, Mara Artibani <sup>1,2,6</sup>, Katherine Nixon <sup>3</sup>, Jennifer Ploski <sup>3</sup>, Laura Santana Gonzalez <sup>1,2</sup>, Abdulkhaliq Alsaadi <sup>1,2</sup>, Nina Wietek <sup>1,2</sup>, Stephen Damato <sup>7</sup>, Sunanda Dhar <sup>7</sup>, Sarah Blagden <sup>5</sup>, Christopher Yau <sup>8,9</sup>, Joanna Hester <sup>10</sup>, Ashwag Albukhari <sup>11</sup>, Eric O. Aboagye <sup>12</sup>, Christina Fotopoulou <sup>3,\*</sup>, Ahmed A. Ahmed <sup>1,2,\*</sup>

1 MRC Weatherall Institute of Molecular Medicine, University of Oxford, Oxford, OX3 9DS, United Kingdom

2 Nuffield Department of Women's and Reproductive Health, University of Oxford, Oxford, OX3 9DU, United Kingdom

3 Division of Cancer, Department of Surgery and Cancer, Imperial College London, W12 0NN, United Kingdom.

4 School of Life Science, Peking University, Beijing 100871, China

5 Department of Oncology, University of Oxford, Oxford OX3 7DQ, United Kingdom

6 Gene Regulatory Networks in Development and Disease Laboratory, MRC Weatherall Institute of Molecular Medicine, Radcliffe Department of Medicine, University of Oxford, Oxford OX3 9DS, United Kingdom

7 Department of Histopathology, Oxford University Hospitals, Oxford OX3 9DU, United Kingdom

8 Division of Informatics, Imaging and Data Sciences, Faculty of Biology Medicine and Health, The University of Manchester, Manchester M13 9PT, UK

9 Alan Turing Institute, London NW1 2DB, UK

10 Transplantation Research and Immunology Group, Nuffield Department of Surgical Sciences, John Radcliffe Hospital, University of Oxford, Oxford OX3 9DU, UK

11 Biochemistry Department, Faculty of Science, King Abdulaziz University, Jeddah, Saudi Arabia

12 Cancer Imaging Centre, Department of Surgery and Cancer, Faculty of Medicine, Imperial College  
London, London, W12 0HS, UK

# These authors contributed equally

\* Corresponding authors and shared senior authorship

## **Running title**

OxC accurately identified poor prognosis in ovarian cancer

## **Corresponding authors**

Christina Fotopoulou: Division of Cancer, Department of Surgery and Cancer, Imperial College  
London, W12 0NN, United Kingdom. c.fotopoulou@imperial.ac.uk

Ahmed Ashour Ahmed: MRC Weatherall Institute of Molecular Medicine, University of Oxford,  
Oxford, OX3 9DS, United Kingdom; Nuffield Department of Women's and Reproductive Health,  
University of Oxford, Oxford, OX3 9DU, United Kingdom. ahmed.ahmed@wrh.ox.ac.uk

## **Conflicts of Interest**

A.A.A., Z.H. and C.Y. filed a patent application for the use of the Oxford Classic. C.F. received  
honoraria from Astra Zeneca/MSD, Roche, GSK, Sequana and Ethicon.

## **Statement of translational relevance**

Serous ovarian cancer is the most common histological subtype of ovarian carcinoma. Due to substantial genetic heterogeneity, it has been challenging to develop robust prognostic classifications based on molecular stratification of high-grade serous ovarian cancer. We recently defined a gene panel “the OxC” that robustly identifies a poor prognosis EMT-high subtype of HGSOC. Here we demonstrate that the NanoString-based OxC-derived high EMT scores are associated with poor prognosis in ovarian cancer independent of stage, grade, surgical outcome or BRCA1/2 mutation status. These results demonstrate the clinical applicability of the OxC and its significant translational potential to enable future efforts for therapeutic optimization for EMT-high tumors.

## **Abstract**

### **Purpose:**

Using RNA-seq, we recently developed the 52-gene-based Oxford Classifier of Carcinoma of the Ovary (Oxford Classic, OxC) for molecular stratification of serous ovarian cancers (SOCs) based on the molecular profiles of their cell-of-origin in the fallopian tube epithelium. Here, we developed a 52-gene NanoString panel for the OxC to test the robustness of the classifier.

### **Experimental Design:**

We measured the expression of the 52 genes in an independent cohort of prospectively collected SOC samples (n = 150) from a homogenous cohort who were treated maximal debulking surgery and chemotherapy. We performed data mining of published expression profiles of SOCs and validated the classifier results on tissue arrays comprising 137 SOCs.

### **Results:**

We found evidence of profound non-genetic heterogeneity in SOC. ~20% of SOCs were classified as epithelial-mesenchymal-transition-high (EMT-high) tumors, that were associated with poor survival. This was independent of established prognostic factors such as tumor stage, tumor grade and residual disease after surgery (HR = 3.3, p = 0.02). Mining expression data of 593 patients revealed a significant association between the EMT scores of tumors and the estimated fraction of alternatively

1 activated macrophages (M2) ( $p < 0.0001$ ) suggesting a mechanistic link between immunosuppression  
2 and poor prognosis in EMT-high tumors.

3 **Conclusions:**

4 The OxC-defined EMT-high serous ovarian cancers carry particularly poor prognosis independent of  
5 established clinical parameters. These tumors are associated with high frequency of  
6 immunosuppressive macrophages suggesting a potential therapeutic target to improve clinical  
7 outcome.



# 1 Introduction

2 More than ninety percent of serous ovarian carcinoma (SOC) cases are high-grade, a highly lethal  
3 gynecological malignancy (1). The treatment regimen for high-grade SOC (HGSOC) consists of a  
4 combination of maximal effort debulking surgery and systemic anticancer cytotoxic and targeted  
5 agents. Recent advances support the use of PARP inhibitors for the treatment of HGSOCs,  
6 particularly those with BRCA1/2 mutations (2). However, the lack of robust and clinically reliable  
7 molecular classifications for non-BRCA1/2-mutated SOC has hindered our ability to accurately  
8 predict patient prognosis or to introduce rationalized therapies. In contrast, clinically established  
9 molecular classification algorithms have been leveraged in other cancers in spite of inconsistencies in  
10 findings (3). Our approach is different in that our classification is driven by subtyping of the cells of  
11 origin. This approach avoids the heterogeneity introduced by genomic alterations in cancer and is,  
12 therefore, more likely to produce a stable classification.

13  
14 In ovarian cancer, several attempts have been made to generate an accurate and clinically applicable  
15 molecular classification that correlated with prognosis. The seminal system developed by The  
16 Australian Ovarian Cancer Study (AOCS) is based on gene expression profiles, which identified a  
17 poor-prognosis mesenchymal subtype, which was subsequently validated by The Cancer Genome  
18 Atlas (TCGA) study (4-6). This system relies on the clustering of transcriptomes and, thus, is apt to  
19 being disturbed by the noise of high-dimensional data. Another limitation of this classifier is the  
20 discrete readout, while the transcriptomic spectrum is likely continuous. Moreover, genomic profiling  
21 of ovarian cancers revealed seven molecular subtypes based on point mutations and structural  
22 aberrations that would likely confound tumor gene-expression based analysis (7,8). Therefore, the  
23 approach to stratify patients with HGSOC into molecular subtypes that associate with clinical  
24 outcome lacks robustness (9), likely owing to substantial intratumor genetic and non-genetic  
25 heterogeneity (10,11). Recent advances in computational algorithms to deconvolute bulk tumors  
26 based on their DNA methylation (12,13), DNA copy number (14) or RNA level profiles (15) are  
27 promising tools for molecular stratification. However, most expression-based deconvolution methods

are limited by the requirement of prior knowledge of the number of tumor compartments and/or their gene expression profiles (16).

To address the aforementioned limitations, our recent work (17) developed a 52-gene panel termed the Oxford Classifier of Carcinoma of the Ovary (Oxford Classic, OxC) (Figure 1A), which estimated the proportions of five molecular signatures (differentiated, KRT17, epithelial-mesenchymal transition [EMT], cell cycle and ciliated) in each bulk tumor. The OxC was derived from single-cell RNA-Seq data of the normal fallopian tube epithelium (FTE), the putative site of origin of SOC (18), based on the hypothesis that the molecular subtypes of normal cells-of-origin could be reflected in the derived SOC subtypes. Thus, the first advantage of the OxC is that it is not confounded by the SOC genomic complexity. The conceptual basis of OxC is that any given tumor can be indicated by a mixture of these molecular signatures, which has been validated in our previous work. The percentage of each signature, i.e. scores, can be estimated by a deconvolution algorithm (19). The robustness of the OxC prognostic correlation was demonstrated by our previous finding that tumors with high EMT scores (i.e. EMT-high tumors) were significantly associated with poor overall survival in seven independent and publicly available datasets, including the TCGA (4) and AOCS (6) datasets. Another advantage of OxC is the improved sensitivity for identifying the EMT-high subtype. Importantly, our recent work reported that the OxC-measured EMT scores identified a group of EMT-high tumors with poor prognosis that were previously defined as non-mesenchymal subtypes using previously reported classification models (17). A further advantage of the OxC is the dependence on only fifty-two genes. This can potentially lead to a more simplified and clinically feasible experimental procedure, which we will investigate in this work.

Another common reason for the failure of translation of molecular stratification of cancers to clinical application is the lack of homogeneity of the cohorts from which such stratifications are derived or subsequently tested. In ovarian cancer, a common source accounting for such lack of homogeneity is the variation in surgical practice and the biases introduced by suboptimal surgical quality, which inevitably makes the assessment of molecular classifications highly challenging. To overcome these

biases, we aimed to validate our developed prognostic panel on a cohort of patients with SOC who had their surgery at a tertiary gynecological cancer center that is recognized by the European Society of Gynaecological Oncology as Centre of Excellence for Ovarian Cancer Surgery with strictly applied criteria (20). This enabled us to significantly reduce the confounding effects of surgical practice variation on patients' survival.

NanoString (21) utilizes barcoding and imaging techniques to obtain absolute quantification of transcripts and enables customized measurement of selected genes. The application of NanoString on clinical samples has the advantage of requiring low input RNA with no amplification steps and this, therefore, ensures accuracy. We constructed a 52-gene NanoString panel to validate the robustness of the OxC (17) on an independent cohort of SOC. We first tested the ability of the 52-gene panel to classify tumors into the five previously described subtypes. We further verified the association between EMT-high tumors and poor prognosis. Finally, we investigated the ability of the ciliated cell markers to distinguish low-grade SOC and validated the results further using immunohistochemistry.

## **Materials and Methods**

### **Patient cohort**

Patients included in the Hammersmith Hospital (HH) cohort were treated at Imperial College London NHS Trust, Hammersmith Hospital, between June 2004 and October 2017. All procedures involving human participants were performed in accordance with the ethical standards of the institutional and/or national research committee and with the principles of the 1964 Declaration of Helsinki and its later amendments or comparable ethical standards. The project was performed under the Hammersmith and Queen Charlotte's and Chelsea Research Ethics Committee approval 05/QO406/178, and frozen tissues supplied by the Imperial College Healthcare NHS Trust Tissue Bank, following full written informed patient consent. All methods were performed in accordance with the relevant guidelines and regulations. Patient demographics were collected retrospectively and are summarized in Table 1.

Staging was defined according to FIGO-criteria for epithelial ovarian cancer (22). Patients were selected for this study according to the following criteria 1) diagnosis of SOC; 2) patients were treated with primary cytoreductive surgery; 3) patients had received platinum-based chemotherapy following primary surgery; 4) tumor samples were snap frozen and banked following primary surgery. Patients were excluded if they had a previous malignancy, had received neo-adjuvant chemotherapy, or tumor tissues had low tumor cellularity. Tumor cellularity for tissues was reviewed by gynae-pathologists based in the West London Gynae Cancer Centre at Hammersmith Hospital, Imperial College Healthcare NHS Trust.

Patients were evaluated at regular intervals following completion of their surgical and systemic treatment for evidence of disease recurrence. Clinical history, examination and CA-125 (if the pre-operative value was elevated) were performed every 3 months for the first 2 years and then 6-monthly. A CT/MRI-scan was ordered if the above examinations revealed any pathology. An isolated elevation in CA-125 was not regarded as a recurrence.

## **RNA extraction**

RNA was extracted from frozen tissues (n = 150) as previously described (23). A NanoDrop spectrophotometer (Thermo Scientific) was used to measure RNA quality and the Qubit RNA HS Assay Kit (Invitrogen) was used to quantify RNA concentrations.

## **NanoString assay**

The customized NanoString CodeSet, designed based on the OxC (17), was purchased. The assay was performed following the manufacturer's manual for the nCounter XT CodeSet gene expression assays. For the hybridization step of each run, the solution containing 50 ng of total RNA and the master mix was incubated at 65°C for 19 hours. The hybridization solution was loaded into the nCounter SPRINT system. The raw data were processed by using the nSolver Analysis Software (RRID:SCR\_003420) and following the manufacturer's protocol. All 150 samples passed the quality control incorporated in

nSolver. The NanoString expression data were deposited at the Gene Expression Omnibus (GEO, RRID:SCR\_005012; accession: GSE151335).

### **Analysis of NanoString data**

The NanoString data were deconvolved as previously described (17). The reference matrix was composed of five transcriptomic signatures corresponding to four secretory cell states, namely differentiated, KRT17, cell cycle and EMT, as well as the ciliated cell type. The proportions of the five signatures were estimated for each bulk tumor by using the R function downloaded from the CIBERSORT (RRID:SCR\_016955) website (19). The reference matrix for the OxC has been reported previously (17). The estimated proportions were termed as scores. For each tumor, five scores added up to one.

### **Validation of NanoString readout by RNA sequencing**

To validate the correlation between NanoString and RNA-Seq readout, we compared the NanoString data and the matched RNA-Seq data from ten HGSOc samples of the cases recruited under the Gynecological Oncology Targeted Therapy Study 01 (GO-Target-01, Ref #11/SC/0014) approved by South Central - Berkshire Research Ethics Committee and the Oxford Ovarian Cancer Predict Chemotherapy Response Trial (OXO-PCR-01, Ref 12/SC/0404) approved by the South Central Oxford C Research Ethics Committee. Both were conducted in accordance with Declaration of Helsinki. All participants involved in this study were appropriately informed and written informed consent was obtained. Tumor samples were biopsied during diagnostic laparoscopy or debulking surgery, immediately frozen on dry ice and stored at -80°C. Frozen tumor samples were embedded in OCT (NEG-50, Richard-Allan Scientific) and 10 µm sections were taken using a CryoStar cryostat microtome (ThermoFisher Scientific). RNA was extracted from the section scrolls by using the RNeasy Mini (Qiagen) according to the manufacturer's instructions. The libraries were prepared by using KAPA mRNA HyperPrep Kits (Roche) and sequenced on the NextSeq500 platform (Illumina) using 75 bp pair-end reads. The RNA-Seq data were trimmed by Trim Galore (RRID:SCR\_011847),

mapped to UCSC hg19 human genome assembly by STAR (RRID:SCR\_015899) (24) and counted by FeatureCount (25). RNA-Seq data of the ten OXO-PCR samples were deposited at GSE160085. The Pearson correlation coefficients and p values were calculated by R function cor.test.

#### **Survival and association analysis**

Two samples that were outliers in the deconvolution analysis (EMT scores  $\geq 0.95$ ), one sample that was an endometrial serous carcinoma subtype and six samples with missing survival data were filtered out (Figure S1). We performed both uni- and multi-variate survival analysis by using function coxph from R package survival. *t*-test was performed between the EMT scores and the residual disease. We could not perform association analysis with deconvolution results and BRCA status in HH cohort due to the limited number of patients with available BRCA status (Tables 1, S1).

#### **External data source and deconvolution analysis**

TCGA “IlluminaHiSeq UNC” RNA-Seq dataset (version: 2017-10-13) and AffyU133a array data (version: 2017-09-08) were downloaded from the UCSC Xena Data Hub (<https://tcga.xenahubs.net>) (4,26). The AOCS dataset was downloaded from the GEO (accession: GSE9899). Seven microarray datasets were obtained from the R package CuratedOvarianCancer (27-31). Exponential transformation was performed for the log transformed data. The OxC scores of bulk tumors from the public datasets were calculated as previously describe (17). The immune cell proportions were estimated by applying the CIBERSORT algorithm to these RNA expression data in non-log-linear space on the web-based platform using the published LM22 and LM6 signatures (19). The association analysis between the OxC signatures and immune signatures was performed by Pearson’s correlation test (function cor.test in R). The linear regression line was estimated by function lm and plotted by function ggplot2 (RRID:SCR\_014601) in R.

## **BRCA1/2 mutation status analysis**

For the TCGA study (4), the matches data of BRCA status were downloaded from the cBioPortal (RRID:SCR\_014555). We categorized samples with putative driver mutations, deep deletions or both as BRCA1/2-mutated and the ones with neither of those as BRCA1/2-wildtype. To investigate if EMT-high tumors were enriched in a certain BRCA status, we performed *t*-test between the EMT scores of BRCA1/2-mutated cases and the ones of BRCA1/2-wildtype cases by R function `t.test`. To study the prognostic effect of BRCA status and EMT levels, we first performed multivariate survival analysis with continuous EMT scores, stages and BRCA1/2 status. Samples were further dichotomized into EMT-high and EMT-low by the median and survival analysis was conducted on four intersected groups: EMT-high BRCA1/2-mutated, EMT-high BRCA1/2-wildtype, EMT-low BRCA1/2-mutated and EMT-low BRCA1/2-wildtype. To increase the power of this analysis, we repeated the analysis with 316 TCGA cases with clinical information (overall survival and stage), known BRCA1/2 status and microarray data, which contained 70 BRCA1/2-wildtype and 246 BRCA1/2-mutated cases, whilst one case had missing stage information.

## **Immunohistochemistry**

Calcyphosine (CAPS), a calcium-binding protein, is a marker of FTE ciliated cells, which we previously identified by single-cell RNA-Seq and validated by immunohistochemistry and immunofluorescent staining (17). To estimate the strength of the ciliated signature in HGSOC samples, we applied the immunohistochemistry of CAPS on the sections of tumor samples. Formalin-Fixed Paraffin-Embedded (FFPE) tissue microarrays were cut into 2.5 or 4  $\mu$ m sections. The Leica Bond Max autostainer (Leica Microsystems) or Autostainer plus Link 48 (Dako) were used to automatically stain the tissue microarray sections with the anti-CAPS antibody (Sigma-Aldrich, Cat #HPA043520; RRID:AB\_10964138). Standard heat-induced epitope retrieval in retrieval buffer pH 6 was used. Tissue sections were kept at 100°C for 20 min and then incubated with the primary antibody for up to 1 hour. The BOND™ Polymer Refine Detection System (DS9800, Leica

Biosystems) was used to visualize the primary antibody. The stained slides were scanned by the ScanScope AT digital pathology slide scanner (Aperio) at 40× magnification.

### Quantification of CAPS positive cells

QuPath (32) was used to quantify the CAPS positive cells. Tumor cells and stromal cells were manually selected based on their nuclear morphology to train the machine learning algorithm incorporated in QuPath. After ensuring the fidelity of this algorithm, we used it to firstly classify cells into tumor and non-tumor cells. The tumor cells were further classified as low (+), medium (++) and high (+++) based on the strength of the staining by the algorithm (Table S2).

### CAPS expression and tumor grades

A logistic regression model was built to predict the tumor grades using CAPS staining data

$$\log\left(\frac{p(x)}{1-p(x)}\right) = \beta_0 + \beta_1x_1 + \beta_2x_2 + \beta_3x_3$$

in which  $x$  is whether the tumor is low-grade or high-grade, and  $x_1$ ,  $x_2$  and  $x_3$  represents the proportions of tumor cells expressing CAPS at the strength of low, medium and high, respectively.  $p(x)$  denotes the probability of  $x$ . The logistic regression model was trained with R function glm. The Receiver Operating Characteristic (ROC) curve was calculated by R package pROC (33). Each patient had one to four sections analyzed. The 141 low grade TMA samples are from 41 patients: 2 patients had 1 section per patient, 4 had 2 sections per patient, 9 had 3 sections per patient and 26 had 4 sections per patient. The statistical learning process was further performed using the eight-fold cross-validation, which evenly divided the data into eight portions and used one portion (1/8) as the testing set and the rest (7/8) as the training set per validation. This allowed us to test the variance of this model.



## Availability of code

Scripts used to analyze and visualize the data were deposit to the GitHub (<https://github.com/OvarianCancerCell/oxford-classic-paper>) and the Code Ocean.

## Results

### EMT scores correlate with poor survival in SOC

Previously, we demonstrated that the OxC RNA-seq based scores correlate with SOC patient overall survival (17). To test the robustness of the results, we sought to: a) develop a gene panel using an independent platform for measuring RNA expression and b) apply this panel on an independent SOC validation cohort. First, we constructed an OxC-based 52-gene panel using the NanoString platform and confirmed that this panel successfully passed all the required quality control measures. We confirmed that the NanoString readout was significantly correlated to the RNA-Seq read counts in a small set of HGSOC samples for the OxC panel (Pearson's  $r = 0.89-0.95$ , Figure S2). We next identified a cohort of 150 patients (Table 1) who had the following key features: a) clinical data were prospectively collected, b) had proportionately homogenous disease stage (85.3% advanced stage III or IV), grade (83.3% high-grade) and histopathology (149 SOC), c) all had an attempt of maximum debulking surgery with 73.3% achieving no visible residual disease, d) relatively long period of follow up (median ~ 50.1 months, range: 0.1 - 153.7) and a high rate of events (73 patients [51%] died, 94 patients [70%] relapsed). Patients had a median age of 61 (18-90) years. The BRCA status was available (somatic or germline) for only 32% of the patients. All patients postoperatively received at least 4 cycles of platinum-based chemotherapy. Median values of progression-free survival and overall survival (OS) were 18.2 (5.8 – 143.7) months and 48.7 (0.1 – 153.7) months respectively.

The expression level of the 52-gene NanoString panel was estimated from fresh-frozen tumor samples obtained from this cohort (Figure 1B and C). Since RNA-Seq-based OxC stratified SOC into five molecular subtypes (differentiated, KRT17, EMT, cell cycle and ciliated), we tested whether the new

panel was able to reproduce this stratification in our cohort. In this cohort, 121 samples (80.7%) were stratified into one of these five subtypes while 29 samples (19.3%) had a mixed phenotype (Figure 1D). Notably, 16.7% of samples had the EMT-high phenotype. Univariate survival analysis showed that the EMT scores significantly correlated with poor survival and increased the hazard of death by 3.1-fold (Table 2). Accounting for other confounding variables was difficult because the relative homogeneity of the cohort meant that subgroups within the different variables were small. Nevertheless, multivariate analysis using established independent prognostic factors (stage, grade and residual disease) revealed that the EMT scores independently associated with prognosis and increased the hazard of death by 3.0-fold (Table 2). Interestingly, neither grade nor residual disease was significantly associated with prognosis in this multivariate analysis. In addition, there was no significant correlation between EMT scores and residual disease status ( $p = 0.40$  for all stages, and  $p = 0.60$  for late-stage disease, Welch two-sample  $t$ -test). However, this could be attributed to the homogeneity of the cohort resulting in small numbers of subgroups as mentioned earlier. Moreover, multivariate analysis showed that EMT scores were independently associated with progression-free survival ( $p = 0.033$ , hazard ratio = 2.5,  $n = 111$ ; Table S1) independent of stage, grade and residual disease. Because of missing data, we were not able to assess the effect of BRCA1/2 mutation status as a potential confounder in this dataset. Therefore, we conducted an independent analysis on TCGA RNA-Seq data and found that the EMT scores, or the scores of any other signature, were not found to be associated with the BRCA1/2 mutation status (Figure S3A). The EMT score was significantly associated with survival independent from BRCA1/2 mutation status and stage (EMT score:  $p = 0.036$ , hazard ratio = 2.1; Table S3). In addition, examining the interaction between the two variables, revealed that the EMT-high BRCA1/2-wildtype group has the worst overall survival independent from stage ( $p = 0.0016$ , hazard ratio = 1.8, Figure S3B). The results of microarray data with a larger sample size ( $n = 315$ ) further confirmed these findings (Figure S3C, Table S4). Taken together, these results support the idea that the OxC-based EMT scores independently correlated with poor prognosis in SOC.

## EMT scores are significantly associated with the abundance of M2 macrophages

Previous studies have highlighted the association between EMT in tumors and a poor immune response (34,35). Therefore, we examined whether EMT-high scores correlated with features suggestive of an immunosuppressive environment in SOCs. To test this, we estimated the proportion of various immune cell signatures in TCGA data (4) using CIBERSORT (19) and correlated this with OxC defined EMT-high tumors. We first used the LM6 reference matrix (19), which contained the transcriptomic signatures of six cell types including CD8 T cells, CD4 T cells, B cells, neutrophils, natural killer cells and monocytes, to deconvolve the RNA-seq data of the TCGA cohort. The analysis revealed that EMT scores were positively correlated with the estimated proportions of the monocyte signature (Pearson's  $r = 0.25$ ,  $p = 1.3e-05$ , Pearson's product-moment correlation test) (Figure S4A). Tumors with higher EMT scores had significantly higher proportions of monocytes ( $p = 8.021e-12$ , one-sided Welch Two Sample  $t$ -test) (Figure 2A). To investigate which was the most prevalent monocyte subtype, we next conducted the analysis using the LM22 reference matrix (19), which can estimate the proportion of 22 types of immune cells in bulk tumors. Our results showed that EMT-high tumors had significantly higher proportions of M2 macrophages (ratio = 0.23/0.17,  $p$ -value =  $4.093e-05$ , by one-sided Welch Two Sample  $t$ -test) (Figure 2B) but not of M0 or M1 macrophages compared with EMT-low tumors (Figure S4B). Notably, all macrophage marker genes except one were upregulated in the EMT-high tumors (Figure 2C). To test the robustness of the results, we repeated the analysis in a second independent dataset, AOCS (6). This reproducibly showed that EMT-high tumors had significantly higher M2 macrophage proportions compared with EMT-low tumors ( $p = 2e-05$ , by one-sided Welch Two Sample  $t$ -test) (Figures 2D, E). Furthermore, the expression of the key EMT-high tumor marker gene, *SPARC* (17), significantly correlated with the expression of the M2 macrophage marker, *CD163* (36) in the TCGA data and seven additional publicly available ovarian cancer expression datasets ( $p < 0.05$ , Figure S5). These results imply that the association between EMT-high scores and poor survival may be in part due to the abundance of the immunosuppressive M2 macrophages.

## **Ciliated cell scores can efficiently predict the tumor grade of SOC**

An important feature of the OxC-based stratification is the association between the high ciliated subtype scores and low-grade SOC (17). Therefore, we tested whether the new NanoString panel could reproduce these results.

In support of our recent findings, we found that the low-grade tumors had a significantly higher level of ciliated scores in the current cohort (Figure 3A). We next hypothesized that the expression levels of ciliated markers can be used to predict the grade status of SOC. To test this hypothesis, we first performed immunohistochemistry for the ciliated marker, CAPS (17), on tissue microarrays of SOC (n = 141 for low-grade and n = 330 for high-grade, from 137 patients; 1-4 data points per patient). We used automated analysis to quantify the level of CAPS staining into low, medium and high using a machine learning algorithm (32) (Figure 3B, Table S2). We next built a logistic regression model with the proportions of low, medium and high cells as the independent variables and with tumor grades as the response variables. This analysis revealed a strong significant association between CAPS expression level and tumor grade (coefficient = -10.72, p = 1.78e-10, logistic regression analysis). To test the predictive power of the model, we randomly selected 60% of the data to train a model and applied the parameters of the model on the remaining 40% of the data. The ROC curve showed that the CAPS expression level efficiently predicted the tumor grades (The area under the ROC curve [AUC] = 0.817, Figures 3C, S6). To confirm the results, we repeated the analysis by randomly sampling 60% of the data 8 times and tested the predictive power of the obtained models on the remaining 40% of the data. This analysis indicated the stability of the predictive power of the model (AUC median = 0.82, range = 0.66 - 0.91; Figure 3D). These results suggest that the expression of CAPS could be used to assist in determining the grade of SOC.

## **Discussion**

By taking advantage of the comprehensive characterization of FTE at a single-cell level, we previously developed the OxC and validated its prognostic power in eight independent ovarian cancer

1 datasets. In the present study we were able to validate the OxC panel in an independent SOC cohort.  
2 Importantly, we were able to establish the significant prognostic value of the OxC-derived EMT  
3 scores and show that this was independent of other well-established prognostic factors such as grade,  
4 stage and postoperative residual disease. We identified ~20% of SOC's being classified as EMT-high  
5 tumors and hence associated with less favorable overall outcome. We hypothesize that these cases  
6 possibly correlate with the 20% of advanced ovarian cancer patients that have been consistently  
7 shown to have poor prognosis despite optimal treatment and tumor-free surgical outcome (37,38).  
8 EMT-status could potentially become a valuable part of a future algorithm that will tailor surgical  
9 radicality and direct it to those who will benefit most.

10  
11 EMT is defined by a transitional loss of the cellular epithelial phenotype and the acquisition of the  
12 cellular mesenchymal phenotype, which is related to poor prognosis in many cancer types. It has been  
13 established that EMT might directly lead to poor disease outcome by facilitating tumorigenesis and  
14 metastasis (34). Similar to EMT, the abundance of intratumor macrophages has been previously  
15 reported to correlate with patient prognosis. While M1 macrophages exert tumoricidal effects, M2  
16 macrophages possess immunosuppressive properties (39) and, thus, a high M1/M2 ratio seems to be  
17 translated into more favorable outcome (40), as opposed to high CD163+ M2 macrophages, that  
18 correlate with elevated IL6 and IL10 with a shorter relapse-free survival (41). Besides, many studies  
19 have reported the relationship between macrophages and EMT, in which macrophages participate in  
20 EMT induction (42,43). It is thought that mesenchymal-like tumor cells and macrophages can interact  
21 with each other in a paracrine fashion to form a positive feedback loop to facilitate tumor metastasis  
22 (44,45). However, while the correlation between M2 macrophage abundance and poor prognosis has  
23 been reported (40,41), the clinical significance of the link between EMT phenotype and macrophages  
24 has not. This may have been due to the difficulty of accurately classifying EMT-high tumors. In  
25 addition, lower levels of TILs have been reported in cases of high levels of the EMT/mesenchymal  
26 component in HGSOE (4). Taken together, we hypothesize that the association between enriched  
27 EMT signatures and disease outcome might be mediated via an alternative or additional route, i.e. the  
28 immunosuppressive effects of M2 macrophages (46). Although our study on clinical data could not

1 unravel the causal relationship, we highlighted that the EMT and macrophage components are  
2 potentially key players in the immunosuppressive tumor microenvironment of HGSOC in humans.  
3 These putatively druggable components provide insights into development of therapies. While we  
4 envisage that the causal links among EMT, M2 macrophages, immunosuppression and poor survival  
5 can be demonstrated by future work in animal models, our work has highlighted potential  
6 immunotherapeutic strategies that can target macrophages in EMT-high SOC. Our results show that  
7 the OxC-based EMT scores significantly correlate with the signature of M2 macrophages in SOC  
8 suggesting that the relationship and potential interactions between mesenchymal-like tumor cells and  
9 macrophages is clinically relevant.

10  
11 Regarding the intriguing relationships between macrophages and molecular signatures derived from  
12 cell subtypes of origin, we hypothesized that cells in HGSOC “inherit” the cell plasticity from the  
13 normal cells of origin (17). Whether M2 macrophages induce the EMT state or the EMT state results  
14 in higher levels of M2 macrophages will be an important question to be addressed by future work,  
15 while the microenvironmental factors, e.g. extracellular matrix, signaling ligands, metabolic products  
16 or extracellular vesicles, may play an important in the interplay between the EMT signature and the  
17 macrophages in HGSOC. Among the 52 genes in the OxC panel, many genes in the OxC have been  
18 reported to have potential relationship with macrophages. Therefore, we envisage that future work can  
19 focus on characterizing the mechanistic links between OxC genes and macrophages.

20  
21 In this work, we first reported the association between macrophages and EMT based on the estimated  
22 proportions of macrophages using a deconvolution algorithm. Although deconvolution algorithms can  
23 efficiently exploit the existing bulk expression data, their accuracy is sometimes limited (47). More  
24 deconvolution methods are emerging with potential improvement in their performance (48,49).  
25 Downstream validation using gene expression levels is still necessary. Therefore, we validated the  
26 deconvolution analysis by testing the correlation between EMT scores and individual genes that are  
27 used as markers for M2 macrophages. Reassuringly, we found a strong correlation at the individual  
28 gene level.

1  
2 Our findings further confirm that low-grade SOCs express significantly higher levels of markers of  
3 ciliated fallopian tube epithelium including CAPS. This is consistent with the notion that low-grade  
4 tumors are more differentiated than high-grade ones (50). This further validates the concept of  
5 classifying tumors based on the expression level of the normal cell-of-origin. Importantly, our work  
6 reported that immunohistochemistry for CAPS expression can potentially assist the diagnosis of low-  
7 grade tumors. To our knowledge, this association has not been described previously. This finding has  
8 significant translational potential to assist in the diagnosis of low-grade tumors using established and  
9 readily available immunohistochemistry and digital imaging methodology.

10  
11 To summarize, in this study we validated the prognostic predictive power of OxC in an independent  
12 cohort of SOC patients, using a 52-gene NanoString panel. By using a patient cohort with  
13 homogenous treatment quality, we endeavored to eliminate confounding bias that would interfere  
14 with evaluating the prognostic significance of OxC. These findings have important translational  
15 significance for the stratification of patients' care in SOC.

1  
2  
3  
4  
5  
6  
7  
8  
9  
10  
11  
12  
13  
14  
15  
16

## Acknowledgements

The research was supported by Ovarian Cancer Action (A. Ahmed), the Cancer Research UK Oxford Centre (A. Ahmed), Oxford Biomedical Research Centre (BRC), National Institute for Health Research (A. Ahmed) and the National Institute for Health Research (NIHR) Biomedical Research Centre based at Imperial College Healthcare NHS Trust and Imperial College London. C. Fotopoulou and P. Cunnea are supported by the Myrovlytis Trust (C. Fotopoulou, P. Cunnea) and Imperial Health Charity (P. Cunnea). We acknowledge Ms. Nona Rama for help with tumor collection and Katherine Costello for clinical data collection. We acknowledge Dr Mariolina Salio for her suggestions on macrophages. We acknowledge Professor Douglas A. Levine for his advice on BRCA data availability. Tissue samples were provided by the Imperial College Healthcare NHS Trust Tissue Bank. Other investigators may have received samples from these same tissues. The views expressed are those of the author(s) and not necessarily those of the NHS, the NIHR or the Department of Health.



# References

1. Siegel RL, Miller KD, Jemal A. Cancer statistics, 2020. *CA Cancer J Clin. American Cancer Society*; 2020;70:7–30.
2. Lee J-M, Nair J, Zimmer A, Lipkowitz S, Annunziata CM, Merino MJ, et al. Prexasertib, a cell cycle checkpoint kinase 1 and 2 inhibitor, in BRCA wild-type recurrent high-grade serous ovarian cancer: a first-in-class proof-of-concept phase 2 study. *Lancet Oncology*. 2018;19:207–15.
3. Sotiriou C, Pusztai L. Gene-expression signatures in breast cancer. *N Engl J Med*. 2009;360:790–800.
4. Bell D, Berchuck A, Birrer M, Chien J, Cramer DW, Dao F, et al. Integrated genomic analyses of ovarian carcinoma. *Nature. Nature Publishing Group*; 2011;474:609–15.
5. Wang C, Armasu SM, Kalli KR, Maurer MJ, Heinzen EP, Keeney GL, et al. Pooled Clustering of High-Grade Serous Ovarian Cancer Gene Expression Leads to Novel Consensus Subtypes Associated with Survival and Surgical Outcomes. *Clin Cancer Res. American Association for Cancer Research*; 2017;23:4077–85.
6. Tothill RW, Tinker AV, George J, Brown R, Fox SB, Lade S, et al. Novel molecular subtypes of serous and endometrioid ovarian cancer linked to clinical outcome. *American Association for Cancer Research*; 2008;14:5198–208.
7. Wang YK, Bashashati A, Anglesio MS, Cochrane DR, Grewal DS, Ha G, et al. Genomic consequences of aberrant DNA repair mechanisms stratify ovarian cancer histotypes. *Nat Genet. Nature Publishing Group*; 2017;49:856–65.
8. Macintyre G, Goranova TE, De Silva D, Ennis D, Piskorz AM, Eldridge M, et al. Copy number signatures and mutational processes in ovarian carcinoma. *Nat Genet. Nature Publishing Group*; 2018;45:1127–270.
9. Chen GM, Kannan L, Geistlinger L, Kofia V, Safikhani Z, Gendoo DMA, et al. Consensus on Molecular Subtypes of High-Grade Serous Ovarian Carcinoma. 2018;24:5037–47.
10. Bashashati A, Ha G, Tone A, Ding J, Prentice LM, Roth A, et al. Distinct evolutionary trajectories of primary high-grade serous ovarian cancers revealed through spatial mutational profiling. *J Pathol. John Wiley & Sons, Ltd*; 2013;231:21–34.
11. Verhaak RGW, Tamayo P, Yang J-Y, Hubbard D, Zhang H, Creighton CJ, et al. Prognostically relevant gene signatures of high-grade serous ovarian carcinoma. *J Clin Invest. American Society for Clinical Investigation*; 2013;123:517–25.
12. Zheng X, Zhao Q, Wu H-J, Li W, Wang H, Meyer CA, et al. MethylPurify: tumor purity deconvolution and differential methylation detection from single tumor DNA methylomes. *Genome Biol. BioMed Central*; 2014;15:419–13.
13. Zheng X, Zhang N, Wu H-J, Wu H. Estimating and accounting for tumor purity in the analysis of DNA methylation data from cancer studies. *Genome Biol. BioMed Central*; 2017;18:17–14.
14. Carter SL, Cibulskis K, Helman E, McKenna A, Shen H, Zack T, et al. Absolute quantification of somatic DNA alterations in human cancer. *Nature Research*; 2012;30:413–21.

- 1 15. Gong T, Szustakowski JD. DeconRNASeq: a statistical framework for deconvolution of  
2 heterogeneous tissue samples based on mRNA-Seq data. *Bioinformatics*. 2nd ed.  
3 2013;29:1083–5.
- 4 16. Yadav VK, De S. An assessment of computational methods for estimating purity and clonality  
5 using genomic data derived from heterogeneous tumor tissue samples. *Brief Bioinformatics*.  
6 2015;16:232–41.
- 7 17. Hu Z, Artibani M, Alsaadi A, Wietek N, Morotti M, Shi T, et al. The Repertoire of Serous  
8 Ovarian Cancer Non-genetic Heterogeneity Revealed by Single-Cell Sequencing of Normal  
9 Fallopian Tube Epithelial Cells. 2020;37:226–7.
- 10 18. Labidi-Galy SI, Papp E, Hallberg D, Niknafs N, Adleff V, Noe M, et al. High grade serous  
11 ovarian carcinomas originate in the fallopian tube. *Nature Publishing Group*; 2017;8:1093.
- 12 19. Newman AM, Liu CL, Green MR, Gentles AJ, Feng W, Xu Y, et al. Robust enumeration of  
13 cell subsets from tissue expression profiles. *Nat Meth. Nature Publishing Group*; 2015;12:453–.
- 14 20. Fotopoulou C, Concin N, Planchamp F, Morice P, Vergote I, Bois du A, et al. Quality  
15 indicators for advanced ovarian cancer surgery from the European Society of Gynaecological  
16 Oncology (ESGO): 2020 update. *Int J Gynecol Cancer. BMJ Specialist Journals*;  
17 2020;30:436–40.
- 18 21. Geiss GK, Bumgarner RE, Birditt B, Dahl T, Dowidar N, Dunaway DL, et al. Direct  
19 multiplexed measurement of gene expression with color-coded probe pairs. *Nat Biotechnol*.  
20 *Nature Publishing Group*; 2008;26:317–25.
- 21 22. Prat J, FIGO Committee on Gynecologic Oncology. Staging classification for cancer of the  
22 ovary, fallopian tube, and peritoneum. 9 ed. *Int J Gynaecol Obstet*. 2014. pages 1–5.
- 23 23. Lu H, Arshad M, Thornton A, Avesani G, Cunnea P, Curry E, et al. A mathematical-descriptor  
24 of tumor-mesoscopic-structure from computed-tomography images annotates prognostic- and  
25 molecular-phenotypes of epithelial ovarian cancer. *Nature Communications*. 2019;10:764.
- 26 24. Dobin A, Davis CA, Schlesinger F, Drenkow J, Zaleski C, Jha S, et al. STAR: ultrafast  
27 universal RNA-seq aligner. *Bioinformatics*. 2013;29:15–21.
- 28 25. Liao Y, Smyth GK, Shi W. featureCounts: an efficient general purpose program for assigning  
29 sequence reads to genomic features. *Bioinformatics*. 2014;30:923–30.
- 30 26. Goldman M, Craft B, Hastie M, Repečka K, McDade F, Kamath A, et al. The UCSC Xena  
31 platform for public and private cancer genomics data visualization and interpretation [Internet].  
32 bioRxiv. Cold Spring Harbor Laboratory; 2019. page 326470. Available from:  
33 <https://www.biorxiv.org/content/10.1101/326470v6>
- 34 27. Ganzfried BF, Riester M, Haibe-Kains B, Risch T, Tyekucheva S, Jazic I, et al.  
35 curatedOvarianData: clinically annotated data for the ovarian cancer transcriptome. *Database*  
36 (Oxford). 2013;2013:bat013.
- 37 28. Bentink S, Haibe-Kains B, Risch T, Fan J-B, Hirsch MS, Holton K, et al. Angiogenic mRNA  
38 and microRNA gene expression signature predicts a novel subtype of serous ovarian cancer.  
39 Creighton C, editor. *PLoS ONE*. 2012;7:e30269.

- 1 29. Pils D, Hager G, Tong D, Aust S, Heinze G, Kohl M, et al. Validating the impact of a  
2 molecular subtype in ovarian cancer on outcomes: a study of the OVCAD Consortium. *Cancer*  
3 *Sci. John Wiley & Sons, Ltd*; 2012;103:1334–41.
- 4 30. Bonome T, Levine DA, Shih J, Randonovich M, Pise-Masison CA, Bogomolny F, et al. A  
5 gene signature predicting for survival in suboptimally debulked patients with ovarian cancer.  
6 *Cancer Res.* 2008;68:5478–86.
- 7 31. Crijns APG, Fehrmann RSN, de Jong S, Gerbens F, Meersma GJ, Klip HG, et al. Survival-  
8 related profile, pathways, and transcription factors in ovarian cancer. Narod S, editor. *PLoS*  
9 *Med. Public Library of Science*; 2009;6:e24.
- 10 32. Bankhead P, Loughrey MB, Fernández JA, Dombrowski Y, McArt DG, Dunne PD, et al.  
11 QuPath: Open source software for digital pathology image analysis. *Sci Rep. Nature*  
12 *Publishing Group*; 2017;7:16878–7.
- 13 33. Robin X, Turck N, Hainard A, Tiberti N, Lisacek F, Sanchez J-C, et al. pROC: an open-source  
14 package for R and S+ to analyze and compare ROC curves. *BMC Bioinformatics. Fourth.*  
15 *BioMed Central*; 2011;12:77–8.
- 16 34. Shibue T, Weinberg RA. EMT, CSCs, and drug resistance: the mechanistic link and clinical  
17 implications. 2017;14:611–29.
- 18 35. Voon DC, Huang RY, Jackson RA, Thiery JP. The EMT spectrum and therapeutic  
19 opportunities. 2017;11:878–91.
- 20 36. Lau SK, Chu PG, Weiss LM. CD163: a specific marker of macrophages in paraffin-embedded  
21 tissue samples. *Am J Clin Pathol.* 2004;122:794–801.
- 22 37. Harter P, Sehouli J, Lorusso D, Reuss A, Vergote I, Marth C, et al. A Randomized Trial of  
23 Lymphadenectomy in Patients with Advanced Ovarian Neoplasms. *N Engl J Med.*  
24 2019;380:822–32.
- 25 38. Bois du A, Reuss A, Pujade-Lauraine E, Harter P, Ray-Coquard I, Pfisterer J. Role of surgical  
26 outcome as prognostic factor in advanced epithelial ovarian cancer: a combined exploratory  
27 analysis of 3 prospectively randomized phase 3 multicenter trials: by the Arbeitsgemeinschaft  
28 Gynaekologische Onkologie Studiengruppe Ovarialkarzinom (AGO-OVAR) and the Groupe  
29 d'Investigateurs Nationaux Pour les Etudes des Cancers de l'Ovaire (GINECO). *Cancer.*  
30 2009;115:1234–44.
- 31 39. Krishnan V, Schaar B, Tallapragada S, Dorigo O. Tumor associated macrophages in  
32 gynecologic cancers. *Gynecol Oncol.* 2018;149:205–13.
- 33 40. Zhang M, He Y, Sun X, Li Q, Wang W, Zhao A, et al. A high M1/M2 ratio of tumor-  
34 associated macrophages is associated with extended survival in ovarian cancer patients. *J*  
35 *Ovarian Res. BioMed Central*; 2014;7:19–16.
- 36 41. Reinartz S, Schumann T, Finkernagel F, Wortmann A, Jansen JM, Meissner W, et al. Mixed-  
37 polarization phenotype of ascites-associated macrophages in human ovarian carcinoma:  
38 correlation of CD163 expression, cytokine levels and early relapse. *Int J Cancer. John Wiley &*  
39 *Sons, Ltd*; 2014;134:32–42.
- 40 42. Nieto MA, Huang RY-J, Jackson RA, Thiery JP. EMT: 2016. 2016;166:21–45.

- 1 43. Robinson BD, Sica GL, Liu Y-F, Rohan TE, Gertler FB, Condeelis JS, et al. Tumor  
2 microenvironment of metastasis in human breast carcinoma: a potential prognostic marker  
3 linked to hematogenous dissemination. *Clin Cancer Res.* 2009;15:2433–41.
- 4 44. Wyckoff J, Wang W, Lin EY, Wang Y, Pixley F, Stanley ER, et al. A paracrine loop between  
5 tumor cells and macrophages is required for tumor cell migration in mammary tumors. *Cancer*  
6 *Res.* 2004;64:7022–9.
- 7 45. Su S, Liu Q, Chen J, Chen J, Chen F, He C, et al. A positive feedback loop between  
8 mesenchymal-like cancer cells and macrophages is essential to breast cancer metastasis.  
9 *Cancer Cell.* 2014;25:605–20.
- 10 46. Peranzoni E, Lemoine J, Vimeux L, Feuillet V, Barrin S, Kantari-Mimoun C, et al.  
11 Macrophages impede CD8 T cells from reaching tumor cells and limit the efficacy of anti-PD-  
12 1 treatment. *Proc Natl Acad Sci USA.* 2018;115:E4041–50.
- 13 47. Sturm G, Finotello F, Petitprez F, Zhang JD, Baumbach J, Fridman WH, et al. Comprehensive  
14 evaluation of transcriptome-based cell-type quantification methods for immuno-oncology.  
15 *Bioinformatics.* 2019;35:i436–45.
- 16 48. Peng XL, Moffitt RA, Torphy RJ, Volmar KE, Yeh JJ. De novo compartment deconvolution  
17 and weight estimation of tumor samples using DECODER. *Nature Communications.* Nature  
18 Publishing Group; 2019;10:4729–11.
- 19 49. Wang L, Sebra RP, Sfakianos JP, Allette K, Wang W, Yoo S, et al. A reference profile-free  
20 deconvolution method to infer cancer cell-intrinsic subtypes and tumor-type-specific stromal  
21 profiles. *Genome Med. BioMed Central;* 2020;12:24–22.
- 22 50. Diaz-Padilla I, Malpica AL, Minig L, Chiva LM, Gershenson DM, Gonzalez-Martin A.  
23 Ovarian low-grade serous carcinoma: a comprehensive update. *Gynecol Oncol.* 2012;126:279–  
24 85.
- 25

## 1 Tables

2 **Table 1.** Summary of Demographics and Clinical Characteristics of Patients in the HH cohort.

<i>Feature</i>	<i>All patients (150)</i>	<i>%</i>	<i>After exclusion (141)</i>	<i>%</i>
<b><i>Age (years)</i></b>				
<i>Median</i>	60		60	
<i>Range</i>	18 - 90		18 - 90	
<b><i>Stage</i></b>				
<i>I</i>	8	5.3	8	5.7
<i>II</i>	12	8.0	12	8.5
<i>III</i>	90	60.0	84	59.6
<i>IV</i>	38	25.3	36	25.5
<i>NA</i>	2	1.3	1	0.7
<b><i>Histological subtype</i></b>				
<i>Serous</i>	149	99.3	141	100.0
<i>Endometrial Serous carcinoma</i>	1	0.7	0	0.0
<b><i>Grade</i></b>				
<i>Low</i>	7	4.0	6	4.3
<i>High</i>	125	83.3	117	83.0
<i>NA</i>	18	12.7	18	12.8
<b><i>Biopsy site</i></b>				
<i>Abdominal wall</i>	1	0.7	1	0.7
<i>Omentum</i>	17	11.3	17	12.1
<i>Ovary</i>	113	75.3	107	75.9
<i>Peritoneum</i>	1	0.7	1	0.7
<i>Parametrium</i>	1	0.7	1	0.7
<i>Colon/bowel</i>	3	2.0	3	2.1
<i>Intra renal</i>	1	0.7	1	0.7
<i>Lymph node</i>	1	0.7	1	0.7
<i>Unspecified tumor mass</i>	12	8.0	9	6.4
<b><i>Postoperative residual disease</i></b>				
<i>Tumor-free</i>	110	73.3	106	75.2
<i>Not tumor-free</i>	28	18.7	28	19.9
<i>Unknown</i>	12	8.0	7	5.0
<b><i>BRCA status</i></b>				
<i>Wildtype</i>	34	22.7	34	24.1
<i>BRCA1 mutated</i>	8	5.3	8	5.7
<i>BRCA2 mutated</i>	6	4.0	6	4.3
<i>Unknown</i>	102	68.0	93	66.0

**Table 2.** Uni- and multivariate analysis for overall survival in the HH cohort.

Univariate analysis	Sample size	Hazard ratio	p	CI95 lower	CI95 upper
EMT score (continuous)	141	3.091	<b>0.023</b>	1.17	8.164
Stage (III-IV vs I-II)	140	2.626	<b>0.012</b>	1.238	5.571
Grade (low vs high)	123	0.136	<b>0.049</b>	0.019	0.988
Residual disease (not tumor-free vs tumor-free)	134	1.995	<b>0.013</b>	1.158	3.439
Multi-variate analysis	Sample size	Hazard ratio	p	CI95 lower	CI95 upper
EMT score (continuous)	116	2.991	<b>0.038</b>	1.061	8.430
Stage (III-IV vs I-II)	116	2.635	<b>0.023</b>	1.145	6.062
Grade (low vs high)	116	0.161	0.072	0.022	1.178
Residual disease (not tumor-free vs tumor-free)	116	1.323	0.349	0.736	2.378

Notes:

- CI95: 95% confidence interval.
- The covariates of multi-variate analysis are EMT score (continuous), Stage (III-IV vs I-II), Grade (low vs high), Residual disease (not tumor-free vs tumor-free).

## Figure legends

### **Figure 1. Independent validation of Oxford Classic with NanoString assay in the HH cohort.**

(A) Diagram shows the workflow of developing and validating Oxford Classic in our previous work. (B) Diagram shows the workflow of an independent validation by performing NanoString OxC assay on the Hammersmith Hospital cohort. (C) Heatmap shows the expression profiles measured by the NanoString OxC assay in 150 tumor samples. Each column is a tumor sample, and each row is a marker gene. The color represents the scaled expression levels. The vertical bar next to the gene names shows the signature each gene corresponds to. (D) Stacked barplot shows the deconvolution results of 150 tumor samples. Each column is a tumor sample corresponding to the one in (B). The colors of bars represent the five signatures, and the size of each sub-bar denotes the proportion of a signature in a given tumor. The horizontal bar at the top shows the arbitrary discrete subtypes with the annotation of patient numbers and percentages.

### **Figure 2. EMT-high tumors have higher proportions of the macrophage M2 signature. (A)**

Estimated proportions of monocytes in TCGA EMT-low, -mid and -high tumors. EMT-high tumors tend to have higher proportions of monocytes (EMT-high vs EMT-low; ratio = 0.52/0.36,  $p = 8.02 \times 10^{-12}$ , by one-sided Welch Two Sample  $t$ -test). (B) Estimated proportions of macrophages M2 in TCGA EMT-low, -mid and -high tumors. EMT-high tumors tend to have higher proportions of macrophages M2 (ratio = 0.23/0.17,  $p$ -value =  $4.09 \times 10^{-5}$ , by one-sided Welch Two Sample  $t$ -test). (C) The relationship between EMT scores and expression levels of putative macrophage M2 markers from the LM22 signature in the TCGA data. (D) The distribution of monocyte enrichment in EMT-low, -mid and -high tumors in the AOCS data. Ratio = 0.17/0.07,  $p = 2.81 \times 10^{-5}$ , by one-sided Welch Two Sample  $t$ -test. (E) The distribution of macrophage M2 enrichment in EMT-low, -mid and -high tumors in the AOCS data. Ratio = 0.10/0.05,  $p = 1.97 \times 10^{-5}$  by one-sided Welch Two Sample  $t$ -test.

### **Figure 3. Low-grade tumors tend to express higher levels of ciliated markers. (A) Distribution of**

ciliated scores of low-grade ( $n = 6$ ) and high-grade ( $n = 116$ ) SOC in the HH cohort. Ratio = 0.28/0.1,

1  $p = 0.0024$ , by Welch Two Sample  $t$ -test. (B) Examples depict the identification of CAPS-expressing  
2 tumor cells by QuPath. In right panels, green represents non-tumor cells and blue denote CAPS-  
3 negative tumor cells, while yellow, orange and red denote the CAPS lowly expressing, moderately  
4 expressing and highly expressing tumor cells respectively. Scale bars indicate 20  $\mu\text{m}$ . IHC,  
5 immunohistochemistry. (C) ROC curve of the logistic regression model that uses CAPS  
6 immunohistochemistry data to predict tumor grades. AUC is shown in the figure. (D) The distribution  
7 of AUC in the eight-fold cross-validation. The line represents the kernel density estimation.



Figure 1

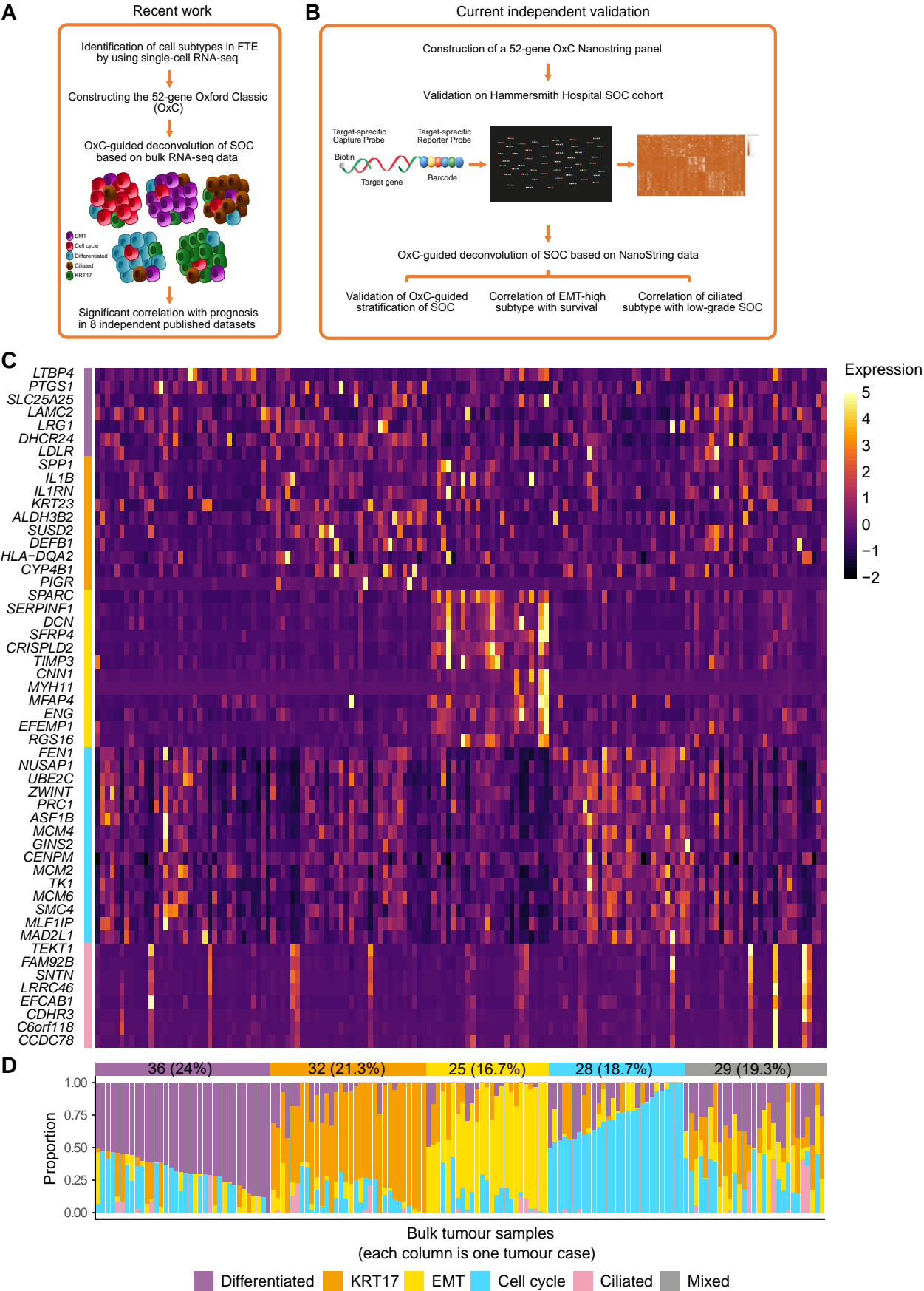
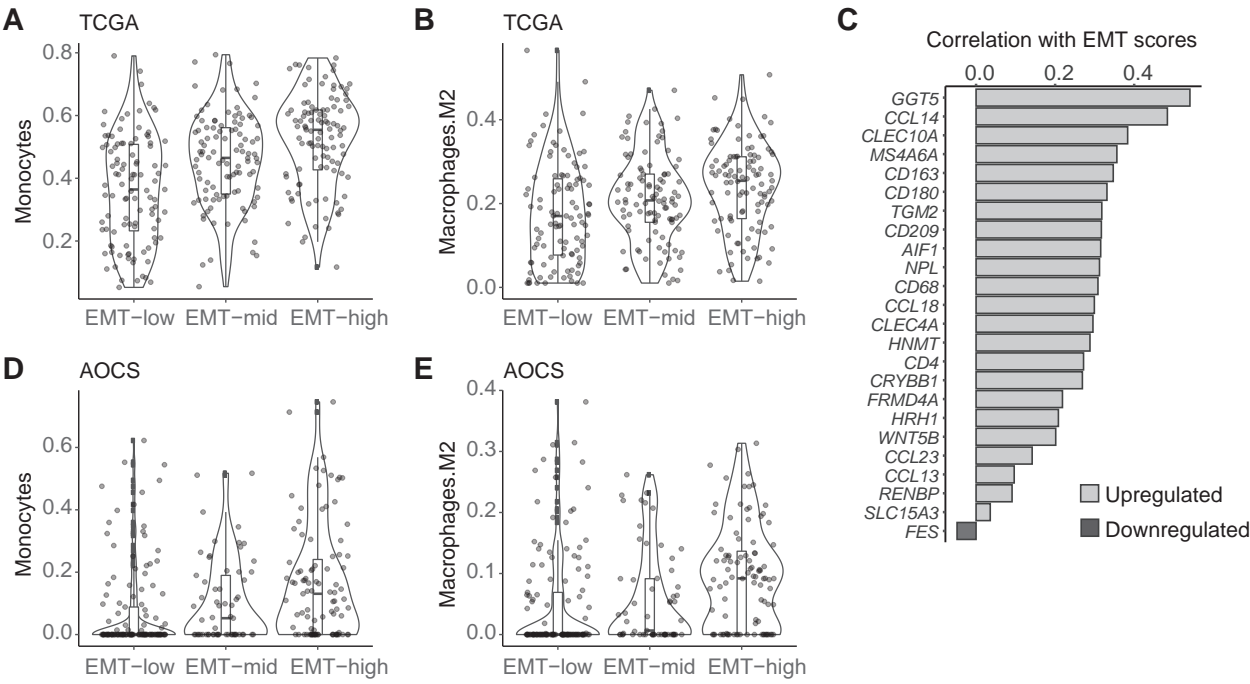


Figure 2



**Figure 3**

